

Electrodeposition and Characterisation of Polypyrroles containing Sulfonated Carbon Nanotubes  
Carol Lynam<sup>1</sup>, Gordon G. Wallace<sup>1</sup>(, David L. Officer<sup>2</sup>

<sup>1</sup> ARC Centre of Excellence for Electromaterials Science,  
Intelligent Polymer Research Institute, University of Wollongong,  
Northfields Avenue, Wollongong, NSW 2522, Australia

<sup>2</sup> Nanomaterials Research Centre and the MacDiarmid Institute for Advanced Materials and  
Nanotechnology, Massey University,  
Private Bag 11222, Palmerston North 5301, New Zealand

Date of Submission: 15<sup>th</sup> May 2006

Date of Acceptance: 18<sup>th</sup> January 2007

Manuscript to be published in the Proceedings of ChemOnTubes.

### **Graphical Abstract**

Using facile diazonium chemistry, sulfonate groups have been covalently attached to single wall carbon nanotubes. It has been shown that pyrrole may be electrochemically polymerised in the presence of these sulfonated single wall carbon nanotubes as dopant ion. The polymerisation results in a conductive, electroactive polypyrrole doped with sulfonated tubes being formed at unusually low potentials. This reduction of polymerisation potential has enabled the formation of a higher activity horse radish peroxidase polymer composite than can be formed with traditional polyelectrolytes, or without supporting electrolyte, thus demonstrating the potential of this composite material as a host matrix for biomolecules.

**Abstract**

Using facile diazonium chemistry, sulfonate groups have been covalently attached to single wall carbon nanotubes. The resulting sulfonated tubes form a stable aqueous dispersion in the presence of pyrrole monomer. Subsequent electropolymerisation results in a conductive, electroactive polypyrrole doped with sulfonated tubes being formed at unusually low potentials. The potential of this material as a host matrix for biomolecules has been demonstrated by entrapping horse-radish peroxidase directly in the polypyrrole during composite formation.

**Keywords:** functionalised carbon nanotubes; single wall carbon nanotubes; conducting polymer; polypyrrole; horse-radish peroxidase.

## Introduction

The unique electronic and mechanical properties of carbon nanotubes (CNTs) have enticed researchers into investigating their use in a variety of composite materials. In particular, conducting polymer-CNT (CP-CNT) composites offer the promise of enhanced polymer electroactivity with significantly improved mechanical strength. Several researchers have used aligned CNT structures as electrodes and electrochemically deposited polypyrrole (Ppy) around the nanotubes in the presence of a supporting electrolyte[?][?]. These aligned Ppy-CNT composite structures have a much higher Young's modulus<sup>1</sup>, charge storage capacitance[?], and improved electrochemical performance[?] including faster response times<sup>3</sup>, than pristine Ppy.

Polypyrrole-single wall carbon nanotube (Ppy-SWNT) nanowires, prepared chemically, using cationic and non-ionic surfactants to disperse the SWNTs, exhibited better electrical properties than pristine Ppy[?][?]. Ppy-CNT composite fibrils approximately 100nm in width were prepared with a conductivity of 16 S cm<sup>-1</sup> compared to 3 S cm<sup>-1</sup> for Ppy itself[?]. ESR spectra of this composite indicated however, that no chemical interaction takes place between the CNTs and Ppy, and that the nanotubes function only as a template during polymerisation. Polypyrrole-multi-walled carbon nanotube (Ppy-MWNT) films, prepared electrochemically from a dispersion of MWNTs in dodecylbenzene sulfonate containing pyrrole, showed nano-scale features due to the MWNTs[?]. Cyclic voltammetry however indicated that the electrochemical activity of these films resulted from Ppy alone, while the conductivity of Ppy with and without the nanotubes was reported as being similar.

Functionalised CNTs have also been used as dopant molecules in Ppy. For example, Ppy-MWNT films were prepared using oxidised MWNTs as dopants[?]. These materials have a higher capacitance than similarly prepared Ppy with more conventional dopants[?][?]. Snook et al. investigated the intercalation behaviour of these Ppy-MWNT films on QCM crystals[?]. Cyclic voltammetry carried out concurrently with QCM measurements indicated that upon oxidation, anion uptake dominated, implying that the oxidised anionic MWNTs only partially doped the polypyrrole.

Given the well-established doping capability of sulfonate groups, we undertook to attach these to CNTs and determine the efficacy of the sulfonated CNTs as a Ppy dopant. Zhou et al. have reported the chemical polymerisation of pyrrole in the presence of sulfonated SWNT bucky paper using iron chloride as the oxidant[?]. This produced a Ppy-bucky paper electrode with a specific capacitance over 6 times higher than pristine bucky paper. We have utilised protocols developed by Dyke et al.[?] to produce sulfonated CNTs and then incorporated these as dopant "molecules" into electrodeposited Ppy films. The use of CNT dopants facilitates the polymerisation of pyrrole at a potential lower than observed for conventional dopant molecules. This facilitated the incorporation of the horse radish peroxidase (HRP) enzyme into the polymer film during synthesis. Additionally, the presence of the functionalised CNTs gave a three-fold increase in the capacitance of the Ppy film.

## Experimental

### 1 Materials

Phosphate buffered saline solution (PBS) was prepared as described elsewhere[?]. All other chemicals, single wall carbon nanotubes (SWNT, HiPCo produced from CNI), sulfanilic acid (Ajax Finechem), sodium nitrate (Aldrich), sulphuric acid (Ajax Finechem), sodium hydroxide

(BDH), acetone (Ajax Finechem), pyrrole (Merck), sodium p-toluene sulfonate (pTS, Merck), sodium polystyrene sulfonate (PSS, Aldrich), sodium chloride (Sigma), 30% (v/v) hydrogen peroxide solution (Merck), horse-radish peroxidase (HRP) (Sigma), 2,2-azino-bis-(3-ethylbenzthiazoline-6-sulfonic acid (ABTS) (Sigma) were used as received.

## **2 Instrumentation**

Electrochemical polymerisation, characterisation and amperometric sensing experiments were performed using an eDAQ e-corder 401 and potentiostat/galvanostat EA 160 with Chart v5.1.2/EChem v2.0.2 software (AD Instruments). BAS CV-27, eDAQ e-corder 401 and potentiostat/galvanostat EA 160 with Chart v5.1.2 software were used for electrochemical quartz crystal microbalance (EQCM) experiments using a Stanford Research Systems EQM 200. Gold coated AT-cut quartz crystal electrodes from Stanford Research Systems, nominal 5 MHz resonant frequency, were used for this investigation.

UV-visible spectra were measured using a Shimadzu 1601 UV-visible spectrophotometer and a 1 cm path length cell. Raman spectra were measured with a Jobin Yvon Horiba HR800 spectrometer using a 632.8 nm laser utilizing a 300-line grating. Scanning electron microscopy (SEM) images were obtained using a Hitachi S900 field emission scanning electron microscope (FESEM). Samples for FESEM were sputter coated with chromium prior to analysis. Electrical conductivity measurements were made with a Jandel Model RM2 four point probe resistivity tester. The elemental analysis was performed with a Carlo Erba Elemental Analyser EA 1108 using a flash combustion technique (Campbell Microanalytical Laboratory, University of Otago, New Zealand). Thermo gravimetric analysis (TGA) was carried out using a Thermo Gravimetric Analyser TGA Q500 (TA Instruments) at a heating rate of 10(/min and air flow (60 mL/min).

## **3 SWNT functionalisation**

Single wall carbon nanotubes were functionalised as described previously<sup>14</sup> using sulfanilic acid as the 4-substituted aniline. Typically SWNTs (60 mg, 5.0 mmol carbon) were stirred with sulfanilic acid (4.0 equiv/mol of carbon), sodium nitrite (4.0 equiv/mol of carbon) and sulphuric acid (4.8 equiv/mol of carbon) as a paste for one hour at 60°C under N<sub>2</sub> to yield SWNT-PhSO<sub>3</sub>Na (Scheme 1). The paste was diluted with acetone and filtered through a PVDF membrane (0.45 µm). The collected solid was washed with acetone until the filtrate became colourless. The resulting black solid was briefly sonicated in dilute aq. NaOH to remove any unreacted sulfanilic acid and the dispersion was filtered through a PVDF membrane (0.45 µm), followed by rinsing with dilute aq. NaOH and water. The solid was dried under vacuum for 2 hours at 60°C to give a product in which 1 in 32 carbons were functionalised by a phenyl sulfonate group according to thermogravimetric analysis

## **4 Electrodeposition of polypyrrole films**

The electro-polymerisation of pyrrole was carried out on gold-coated mylar and gold-coated indium tin oxide (ITO)-glass, both with a surface area of 1.0 cm<sup>2</sup>, and gold-coated quartz crystals with a surface area of 1.37 cm<sup>2</sup>. Ppy films were grown galvanostatically at 0.25 mA cm<sup>-2</sup> from solutions of 0.2 M (30 mins) and 1.0 M (5 mins) pyrrole respectively in the presence of SWNT-PhSO<sub>3</sub>Na as electrolyte (0.3% w/v), and 0.2 M pyrrole in the presence of 0.2 M pTS or 0.2 M PSS. A platinum mesh auxiliary electrode and Ag/AgCl reference electrode were used. After growth the films were rinsed with de-ionised water and dried under a stream of nitrogen. Post-polymerisation cyclic voltammetry and Electrochemical Quartz Crystal Microbalance (EQCM)

studies were carried out in 0.2 M NaCl with the upper and lower limits being 300 mV and -1100 mV, respectively. Amperometric sensing experiments were performed using a three-electrode electrochemical cell, which comprised a working electrode (polypyrrole film), a platinum mesh auxiliary electrode and an Ag/AgCl reference electrode.

## **Results and Discussion**

Following sulfonation of the SWNTs, the functionalised nanotubes were incorporated into Ppy during electrodeposition and the electrochemical properties of the resultant material were determined. The electrodeposition behaviour and electrochemical properties after growth were compared to those observed with either para toluene sulfonate (pTS) or polystyrene sulfonate (PSS) as dopant.

### ***1 Formation and characterisation of sulfonated single wall carbon nanotubes (SWNT-PhSO<sub>3</sub>Na)***

The procedure described by Dyke for the functionalisation of SWNTs using diazonium chemistry was followed, employing sulfanilic acid as the 4-substituted aniline (Scheme 1)<sup>14</sup>. This reaction produced single wall carbon nanotubes in which 1 in 32 carbons were functionalised by a phenyl sulfonate group according to thermogravimetric analysis (TGA, 22% weight loss of functional groups), with a sulphur content of 5.6 % as determined by elemental analysis. This ratio of functionalisation compares well to that previously documented by Dyke<sup>14</sup>.

The Raman spectrum of the starting raw SWNT material shows a small disorder band (D band) at 1320 cm<sup>-1</sup> (Figure 1) as expected due to the manufacturer's acidic purification treatment, whereas the spectrum of SWNT-PhSO<sub>3</sub>Na shows a significant increase in the disorder mode relative to the tangential mode (G-band at 1590 cm<sup>-1</sup>). This increase in intensity of the D band indicates a significant conversion of sp<sup>2</sup> hybridised carbons in the nanotubes to sp<sup>3</sup>, consistent with a high degree of functionalisation[?]. There is also a change in the radial breathing modes of the functionalised nanotubes when compared to the as-received SWNTs, which is consistent with sidewall functionalisation[?].

The functionalised SWNTs (SWNT-PhSO<sub>3</sub>Na), although not water soluble, were readily dispersed in water, without the need for sonication. SWNT-PhSO<sub>3</sub>Na also dispersed sparingly in ethanol and isopropanol, poorly in 1,2-dichloroethane and DMF, and not at all in DMPU or THF. This contrasts greatly with the SWNT starting material.

The conductivity of bucky paper formed from the SWNT-PhSO<sub>3</sub>Na material was measured to be 4.4 ± 0.9 S cm<sup>-1</sup>, using the standard four point probe method. This is two orders of magnitude lower than has been reported for single wall carbon nanotubes (that had not been functionalised) in a bucky paper format[?]. The loss of electrical conductivity of the functionalised SWNTs is attributed to a high degree of side-wall functionalisation. Measurements of the ionic conductivity of a solution of SWNT-PhSO<sub>3</sub>Na (30 mg SWNT-PhSO<sub>3</sub>Na in 10 ml H<sub>2</sub>O) gave a value of 2.07 μS cm<sup>-1</sup>.

### ***2 Incorporation of sulfonated tubes during Ppy synthesis***

The electrochemical growth and deposition of Ppy on gold-coated mylar, gold-coated ITO-glass and gold-coated quartz crystals was carried out under galvanostatic conditions at a current density

of  $0.25 \text{ mA cm}^{-2}$  in the presence of SWNT-PhSO<sub>3</sub>Na (0.3% w/v) or pTS (Figure 2). In order to determine the effect of pyrrole concentration, solutions containing 0.2 M or 1.0 M pyrrole were employed. A notable feature of the chronopotentiograms in Figure 2 is that the use of either the sulfonated nanotubes or PSS reduced the potential for Ppy deposition by over 150 mV, from  $> 0.6 \text{ V}$  in the case of pTS, to  $< 0.45 \text{ V}$  (Figure 2). Note also that the potential monitored during growth with pTS, PSS or the carbon nanotubes present did not increase, indicating formation of a conducting deposit.

Using EQCM it was found that during deposition with either pTS (Figure 2a) or PSS (Figure 2b) as electrolyte, the frequency (mass deposited) changed almost linearly with time. However, employing SWNT-PhSO<sub>3</sub>Na as the electrolyte, a rather curious change in frequency (mass deposited) was observed. The mass change was as expected only over the first few seconds (albeit a more rapid frequency (mass) change than observed with pTS and PSS), it then decreased slightly even though charge continued to be consumed. It was found that this behaviour could be overcome by increasing the pyrrole monomer concentration (Figure 2c) although again a rapid decrease in frequency (increase in mass) was still observed over the initial stages. This may be attributed to several factors: i) depletion of monomer in the vicinity of the electrode, ii) slow diffusion of pyrrole monomer through the nanotube dispersion to the electrode surface, iii) the polymerisation of pyrrole in the presence of SWNT-PhSO<sub>3</sub>Na results in the formation of a more soluble/dispersible product that does not deposit on the electrode. In order to overcome these effects the use of a higher concentration, 1.0 M pyrrole rather than 0.2 M pyrrole, was investigated. This did result in more typical polymer deposition profiles being obtained from the EQCM. However, the rate of deposition and the final mass deposited (final frequency change) was still less than when pTS or PSS was used as the dopant. In a further experimental set up, the use of an electrode that was pre-coated with a thin (30  $\mu\text{m}$ ) layer of Ppy-pTS was considered. An almost linear change in frequency (mass deposited) with time was observed when the Ppy-pTS electrode was used in conjunction with 1.0 M pyrrole in the deposition bath (Figure 2e). It is well known that monomer oxidises more readily on deposited polymer than on a bare metal surface.

With respect to morphology, the effect of the nanotubes in the Ppy-SWNT-PhSO<sub>3</sub>Na film can be clearly observed using SEM (Figure 3). Small bundles of SWNTs which appear to be coated with polymer are apparent (Figure 3c). There are no discrete domains, rather a random network of nanotube bundles. Ppy-pTS films however have a very different morphology (Figure 3a), and appear denser than the Ppy-SWNT-PhSO<sub>3</sub>Na films. Ppy-PSS films have a very smooth surface (Figure 3b), confirming that the nanostructure observed in the Ppy-SWNT-PhSO<sub>3</sub>Na films is due to the presence of the functionalised carbon nanotubes.

Raman spectra obtained from Ppy-SWNT-PhSO<sub>3</sub>Na films (Figure 4) show the presence of polypyrrole and SWNTs. The peaks at  $933 \text{ cm}^{-1}$  and  $1086 \text{ cm}^{-1}$  have been associated with the bipolaron structure and those at  $970 \text{ cm}^{-1}$  and  $1059 \text{ cm}^{-1}$  with the polaron structure<sup>8</sup>. The spectra confirm that after growth the films are in the oxidised state due to the ratio of bipolaron: polaron bands (1.07 for Ppy-pTS, 1.05 for Ppy-PSS and 1.13 for Ppy-SWNT-PhSO<sub>3</sub>Na).

The UV-spectra obtained for both Ppy-pTS and Ppy-PSS films (Figure 5) are typical of polypyrrole with peaks at 480 nm corresponding to the polaron/bipolaron state and a shoulder extending into the near-IR indicative of the free carrier tail in conducting polymers[?]. The

spectrum obtained for Ppy containing the carbon nanotubes and prepared from 0.2 M pyrrole is indicative of oligomer formation, with low intensity absorbance bands at 600 nm and 930 nm[?]. Ppy-SWNT-PhSO<sub>3</sub>Na prepared from 1.0 M pyrrole however shows a peak at 400 nm and a broad shoulder at 890 nm. This would indicate that even for films grown from 1.0 M pyrrole the polymer is not fully doped.

Electrical conductivity measurements were carried out on stand-alone Ppy-pTS and Ppy-SWNT-PhSO<sub>3</sub>Na films (prepared from 0.2 M pyrrole) using the standard four point probe method. The room temperature conductivities were measured to be  $94 \pm 17 \text{ S cm}^{-1}$  for Ppy-pTS and  $0.5 \pm 0.26 \text{ S cm}^{-1}$  for Ppy-SWNT-PhSO<sub>3</sub>Na. This much lower conductivity is consistent with oligomer formation as observed in the UV-spectra.

### **3 Electrochemical properties of deposited polymer**

After growth, the Ppy films were rinsed in water and then transferred into a 0.2 M NaCl solution, and cyclic voltammograms recorded. Figure 6 shows the behaviour of the Ppy-SWNT-PhSO<sub>3</sub>Na film when cycled between 0.3 V and -1.0 V. The CV is typical of polypyrrole; however several important differences can be seen between this CV and that for Ppy-pTS. The peak potentials of the Ppy-SWNT-PhSO<sub>3</sub>Na film are more negative than those of the Ppy-pTS film. The output current of the Ppy-SWNT-PhSO<sub>3</sub>Na film is three times higher than that of the Ppy-pTS film, probably due to the capacitive nature of the SWNTs incorporated within the film. The capacitance of all the Ppy films was calculated to be  $18 \text{ mF cm}^{-2}$  for Ppy-PSS and  $30 \text{ mF cm}^{-2}$  for Ppy-pTS, while the capacitance of the Ppy-SWNT-PhSO<sub>3</sub>Na film was at least three times higher at  $90 \text{ mF cm}^{-2}$ .

In order to confirm that SWNT-PhSO<sub>3</sub>Na had indeed doped the polymer, post-polymerisation cyclic voltammetry was carried out on the composite film using EQCM. Polypyrrole films were prepared from 0.2 M pyrrole with PSS, pTS or SWNT-PhSO<sub>3</sub>Na as counterions. PSS is a polyelectrolyte that is expected to behave in a similar manner to SWNT-PhSO<sub>3</sub>Na, whereas pTS is a much smaller anion, which is free to leave the polymer matrix. Upon oxidation and reduction of Ppy-pTS, mass changes corresponding to both chloride anion and sodium cation movement were seen as expected (not shown).

With PSS as counterion, a mass increase upon reduction of Ppy was obtained, with a corresponding mass decrease upon oxidation (see Figure 7a). This can be explained by the fact that the movement of positively charged sodium ions into the polymer predominates in neutralising the excess anionic sulfonate groups on the immobile PSS dopant upon polymer reduction. During oxidation the mass decreased due to expulsion of the sodium cations.

In an analogous fashion, a mass decrease was observed upon oxidation of the Ppy-SWNT-PhSO<sub>3</sub>Na film, with a mass increase seen upon reduction (Figure 7b). In contrast, Ppy-SWNT-PhSO<sub>3</sub>Na prepared from 1.0 M pyrrole is not doped, as evidenced by the mixed anion and cation movement during cyclic voltammetry with in situ QCM measurements (Figure 8a). With respect to the two layered film structure prepared from 1.0 M pyrrole, a similar trend emerged, (Figure 8c).



#### **4 Incorporating Enzyme into Ppy-SWNT-PhSO<sub>3</sub>Na film for use in Biosensing**

The low polymerisation potential observed for pyrrole in the presence of SWNT-PhSO<sub>3</sub>Na led us to investigate the possibility of trapping biomolecules [horse radish peroxidase (HRP)] into the polypyrrole-CNT matrix. This was achieved during polymer synthesis and the use of the biocomposite for biosensing was then investigated. The concentration of HRP and SWNT-PhSO<sub>3</sub>Na in the polymerisation solution was 0.02% and 0.3% respectively w/v. The polymerisation was carried out galvanostatically at a current density of 0.25 mA cm<sup>-2</sup> for 15 minutes on gold mylar. Polymerisation of pyrrole in the presence of SWNT-PhSO<sub>3</sub>Na and HRP occurred at a slightly higher potential than with SWNT-PhSO<sub>3</sub>Na alone. This may be due to the insulating nature of the enzyme, which increased the resistance of the polymerisation solution. The post polymerisation cyclic voltammogram of the Ppy-SWNT-PhSO<sub>3</sub>Na-HRP film in sodium chloride solution was identical to a Ppy-SWNT-PhSO<sub>3</sub>Na film without HRP. The absolute mass of the enzyme immobilised within the Ppy-SWNT-PhSO<sub>3</sub>Na-HRP film was determined by a colorimetric enzyme assay [?], and was calculated to be  $2.6 \times 10^{10}$  molecules. In comparison, polypyrrole prepared under identical conditions but with PSS as dopant and without electrolyte had  $2.3 \times 10^{10}$  and  $2.0 \times 10^{10}$  HRP molecules immobilised respectively.

The amperometric ( $E_p = -100$  mV vs. Ag/AgCl) response of Ppy-SWNT-PhSO<sub>3</sub>Na-HRP in phosphate buffered saline (pH 7.4) to the addition of 2 mmol dm<sup>-3</sup> H<sub>2</sub>O<sub>2</sub> is shown in Figure 9. Upon addition of H<sub>2</sub>O<sub>2</sub>, the current increased sharply by 83  $\mu$ A cm<sup>-2</sup>. The response obtained from the Ppy-SWNT-PhSO<sub>3</sub>Na-HRP film confirms the electrochemical activity of HRP which was immobilised within the polypyrrole matrix. In comparison, the current response to H<sub>2</sub>O<sub>2</sub> obtained from a Ppy-HRP film, prepared under identical conditions but with PSS as dopant and without additional electrolyte was 37  $\mu$ A cm<sup>-2</sup> and 3  $\mu$ A cm<sup>-2</sup> respectively. This result, in conjunction with the results from the colorimetric enzyme assay, show that the presence of SWNT-PhSO<sub>3</sub>Na as electrolyte during the polymerisation of pyrrole, allows the incorporation of more active enzyme molecules than with traditional polyelectrolytes, or without supporting electrolyte.

#### **Conclusion**

It has been shown that pyrrole may be electrochemically polymerised in the presence of sulfonated single wall carbon nanotubes as dopant ion. Unusual deposition behaviour was evidenced, which is likely due to limited diffusion of the monomer through the nanotube dispersion and the polyelectrolyte nature of the functionalised carbon nanotubes. Pyrrole polymerisation employing functionalised nanotubes as the electrolyte and dopant results in a composite material comprised of mostly polypyrrole oligomers; as a result the electrical conductivity of the composite is reduced. The polymerisation of pyrrole in the presence of functionalised nanotubes occurred at a potential lower than for more traditional electrolytes. This reduction of polymerisation potential has enabled the formation of a higher activity horse radish peroxidase polymer composite than can be formed with traditional polyelectrolytes, or without supporting electrolyte.

[pic]

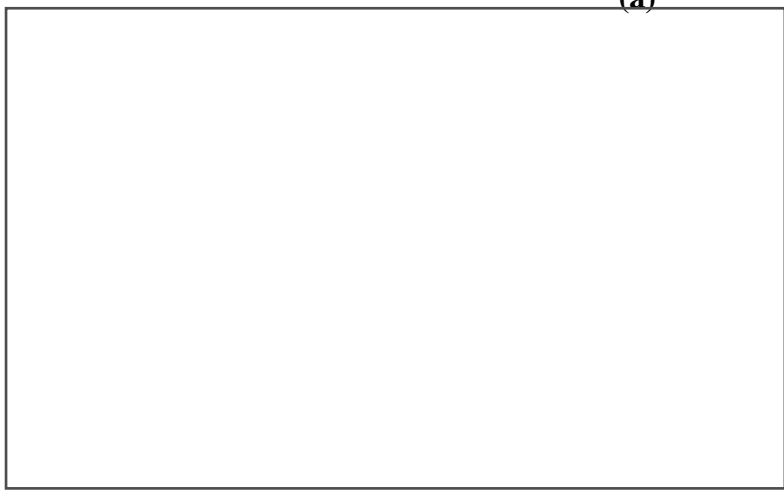
**Scheme 1:** The preparation of SWNTs functionalised with phenyl sodium sulfonate (SWNT-PhSO<sub>3</sub>Na) using sulfanilic acid and nitrous acid.



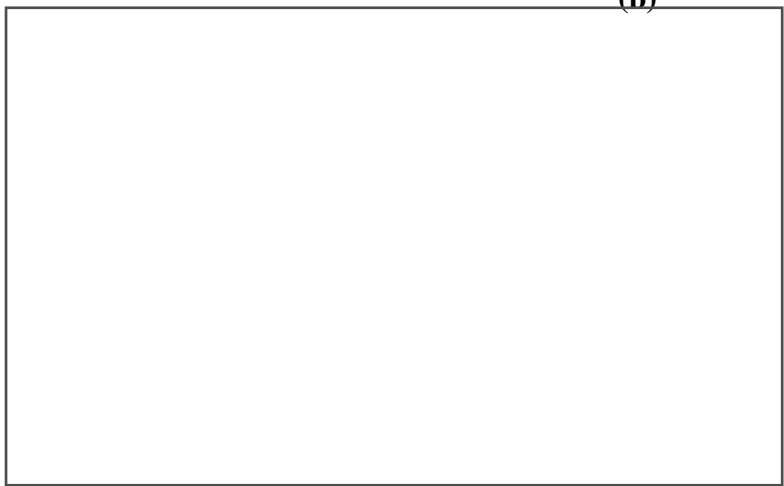
**Figure 1:** Raman spectra of raw SWNT and SWNT-PhSO<sub>3</sub>Na.



**(a)**



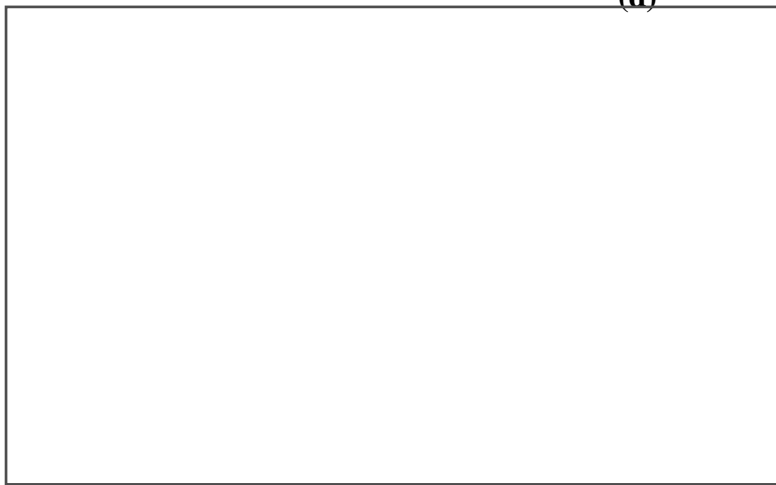
**(b)**



**(c)**

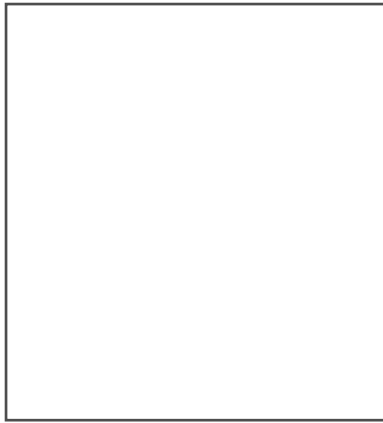


(d)

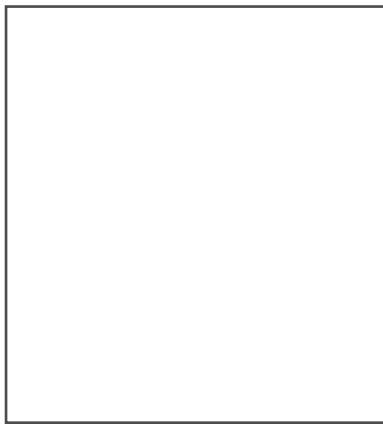


(e)

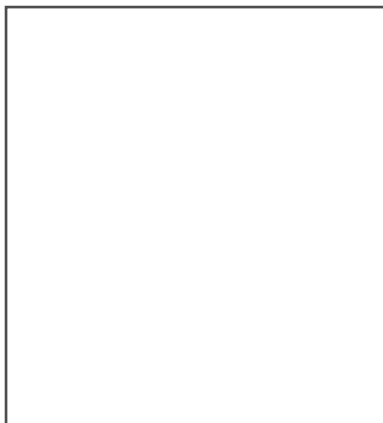
**Figure 2:** Chronopotentiograms of polypyrrole growth and deposition monitored by EQCM (a) Ppy-SWNT-PhSO<sub>3</sub>Na (0.2 M pyrrole), (b) Ppy-PSS (0.2 M pyrrole), (c) Ppy-pTS (0.2 M pyrrole), (d) Ppy-SWNT-PhSO<sub>3</sub>Na (1.0 M pyrrole) and (e) Ppy-SWNT-PhSO<sub>3</sub>Na (1.0 M pyrrole) on a pre-formed Ppy-pTS layer.



**(a)**



**(b)**



**(c)**

**Figure 3:** SEM images of **(a)** Ppy-pTS, **(b)** Ppy-PSS and **(c)** Ppy-SWNT-PhSO<sub>3</sub>Na.

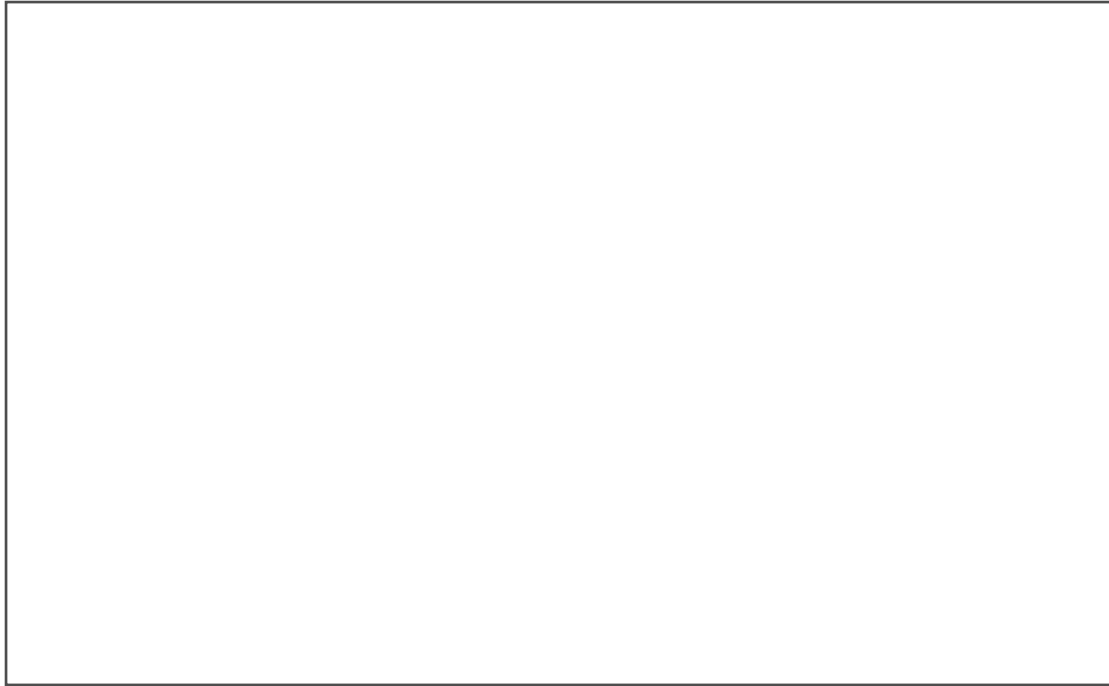


**Figure 4:** Raman spectra of Ppy-SWNT-PhSO<sub>3</sub>Na, Ppy-PSS and Ppy-pTS.

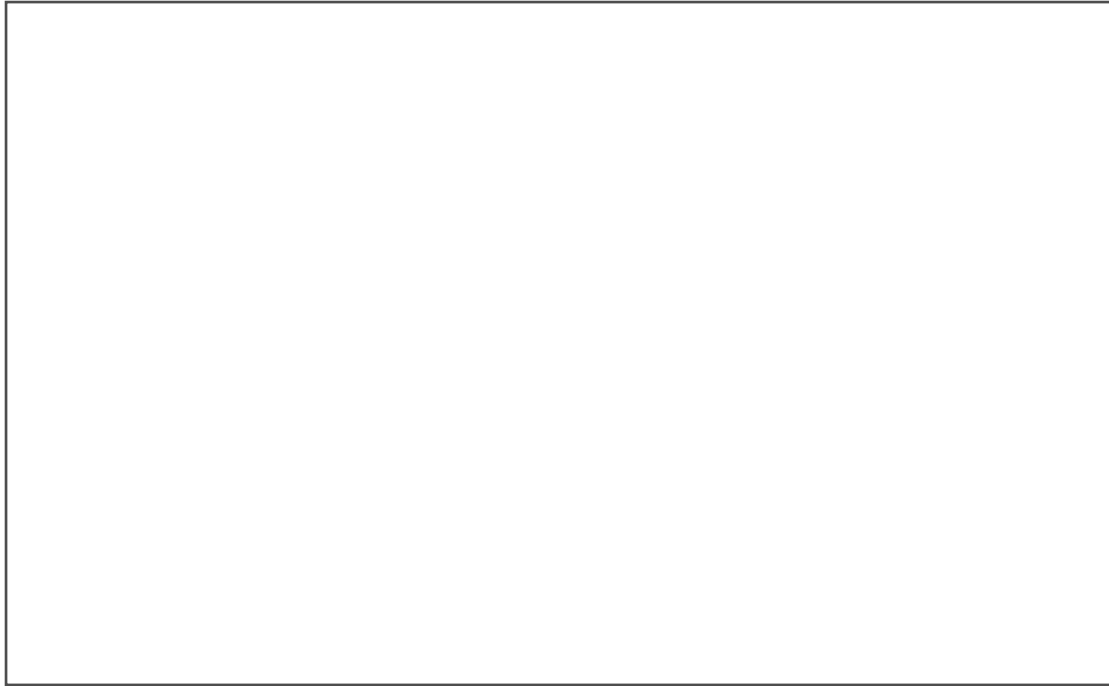


**Figure 5:** UV spectra of Ppy-PSS, Ppy-pTS and Ppy-SWNT-PhSO<sub>3</sub>Na prepared from 0.2 M pyrrole, and Ppy-SWNT-PhSO<sub>3</sub>Na prepared from 1.0 M pyrrole, all grown on gold coated-ITO.



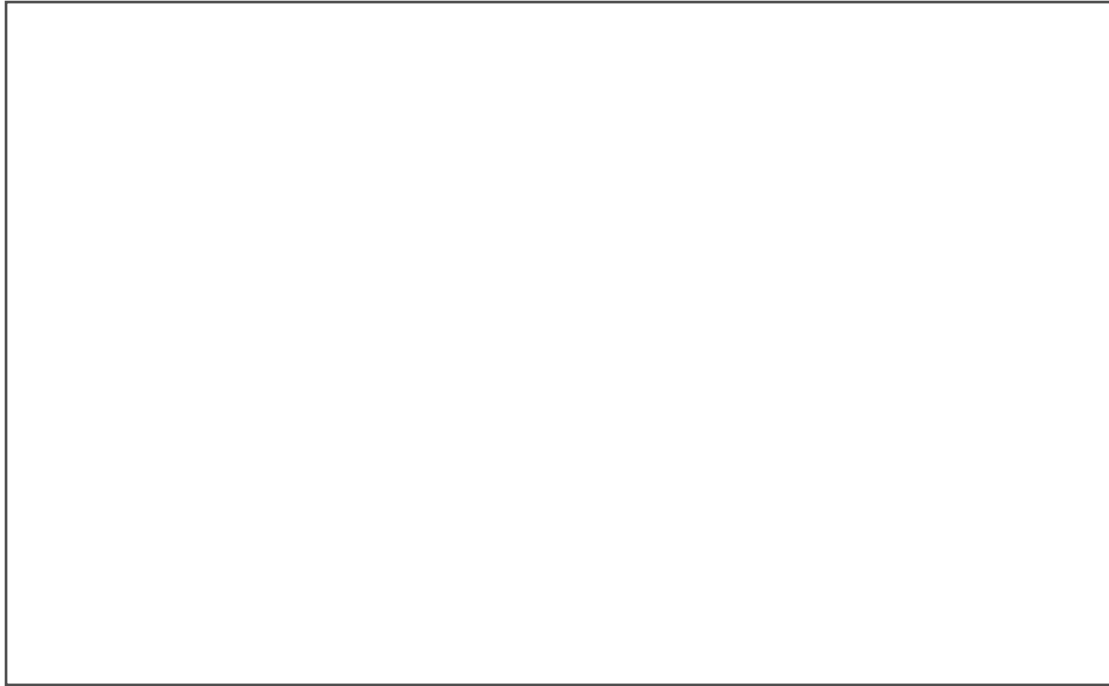
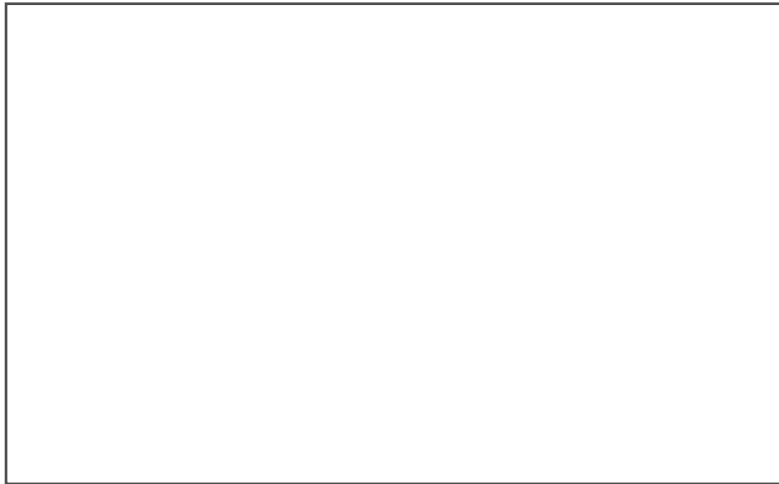
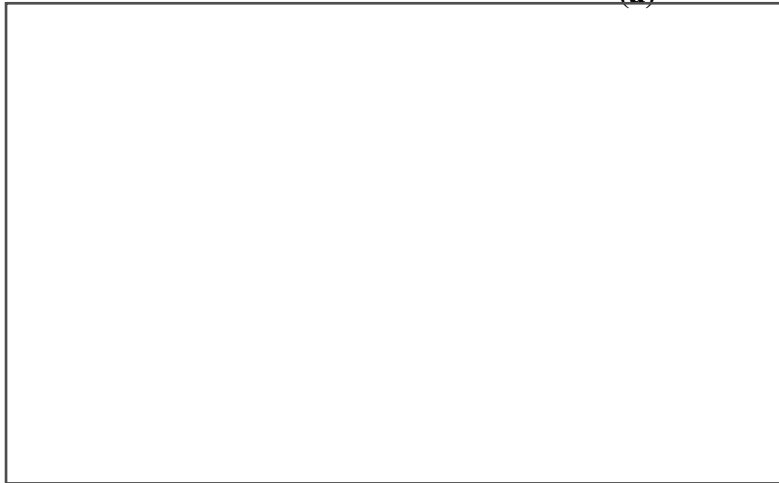


**Figure 6:** Cyclic voltammograms of Ppy-pTS, Ppy-SWNT-PhSO<sub>3</sub>Na and Ppy-PSS films on gold coated quartz crystals at a scan rate of 20 mV s<sup>-1</sup> in 0.2 M NaCl.



(a)

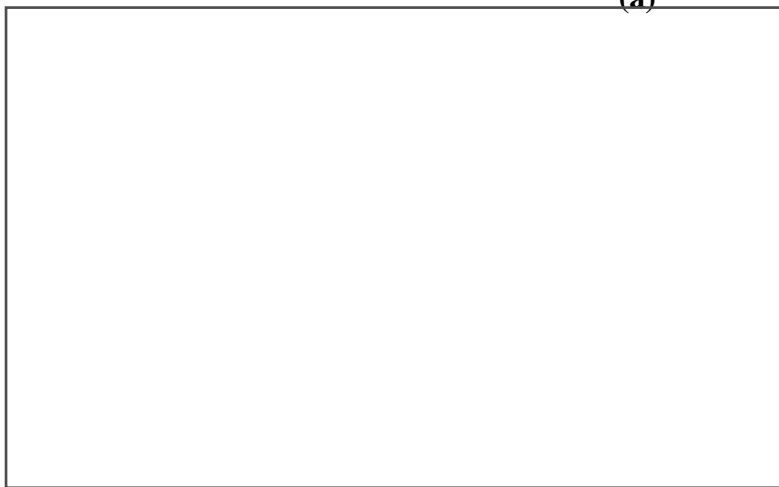


(b)

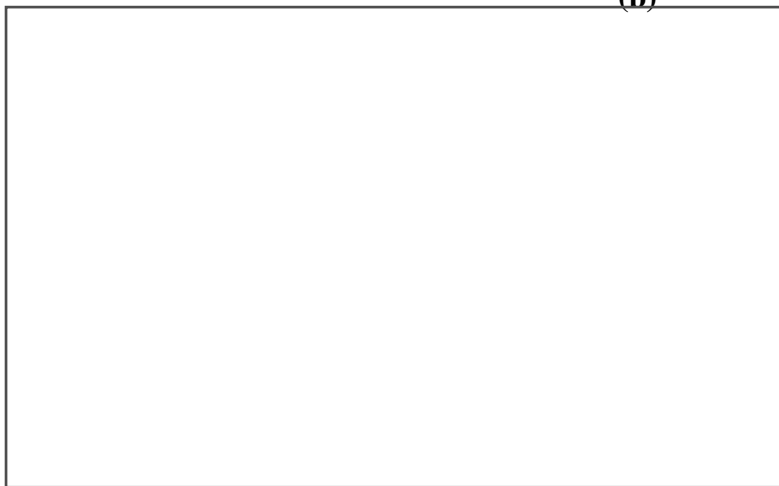
**Figure 7:** Cyclic voltammetric (grey) and EQCM response (black) of (a) Ppy-PSS (0.2 M pyrrole) and (b) Ppy-SWNT-PhSO<sub>3</sub>Na (0.2 M pyrrole) in 0.2 M NaCl, scan rate 20 mV s<sup>-1</sup>.



(a)



(b)



(c)

**Figure 8:** Cyclic voltammetric (grey) and EQCM response (black) of (a) Ppy- SWNT-PhSO<sub>3</sub>Na (1.0 M pyrrole) (b) Ppy-SWNT-PhSO<sub>3</sub>Na (0.2 M pyrrole) on a preformed Ppy-pTS film and (c) Ppy-SWNT-PhSO<sub>3</sub>Na (1.0 M pyrrole) on a preformed Ppy-pTS film in 0.2 M NaCl, scan rate 20 mV s<sup>-1</sup>.

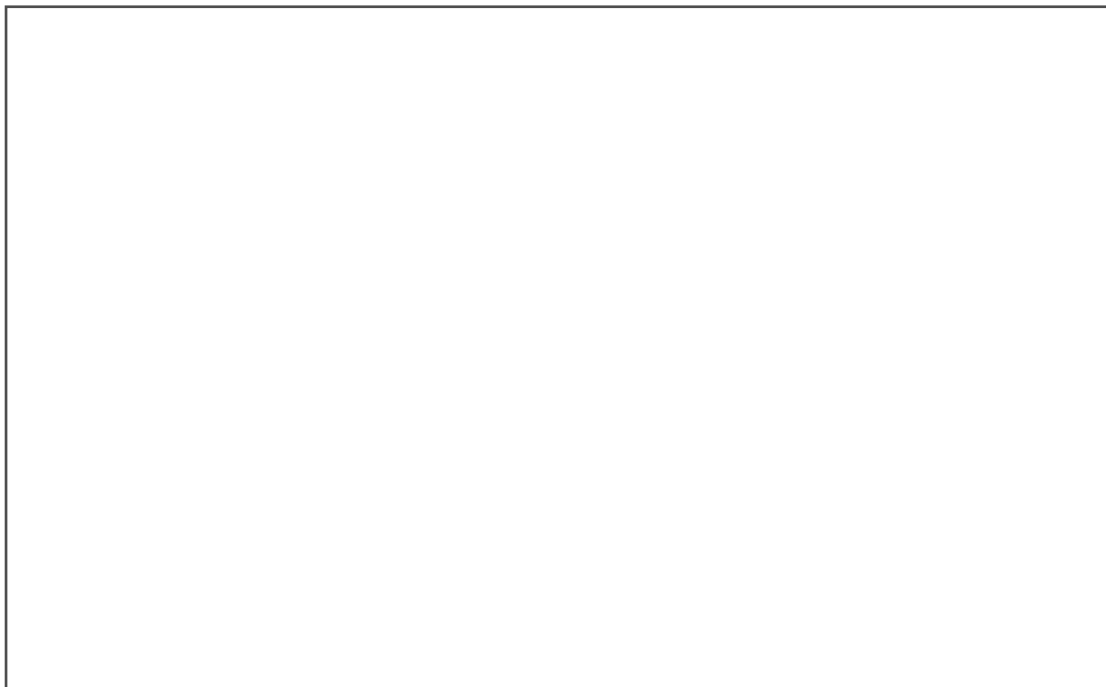


**Figure 9:** Amperometric response of polypyrrole films with HRP and various dopants in the polymerisation solution, to  $\text{H}_2\text{O}_2$ .  $E_p = -100$  mV (vs. Ag/AgCl). The experiment was carried out under hydrodynamic conditions. \* Indicates the addition of  $\text{H}_2\text{O}_2$  (final concentration  $2 \text{ mmol dm}^{-3}$ ).

## References:

( Corresponding author: Prof. Gordon G. Wallace  
*ARC Centre of Excellence for Electromaterials Science*  
*Intelligent Polymer Research Institute*  
*University of Wollongong*  
*Northfields Avenue, Wollongong, NSW 2522, Australia.*  
*Fax: 61-2-4221 3114*  
E-mail: gwallace@uow.edu.au

- [i]. M. Gao, S. Huang, L. Dai, G. Wallace, R. Gao and Z. Wang, *Angew. Chem. Int. Ed.* 39, 20, 3664 (2000).
- [ii]. J. H. Chen, Z. P. Huang, D. Z. Wang, S. X. Yang, J. G. Wen and Z. F. Ren, *Appl. Phys. A*, 73, 129 (2001).
- [iii]. M. Hughes, M. S. P. Schaffer, A. C. Renouf, C. Singh, G. Z. Chen, D. J. Fray and A. H. Windle, *Adv. Mater.* 14, 5, 382 (2002).
- [iv]. J. H. Chen, Z. P. Huang, D. Z. Wang, S. X. Yang, W. Z. Li, J. G. Wen and Z. F. Ren, *Synth. Met.* 125, 289 (2002).
- [v]. X. Zhang, J. Zhang, R. Wang, T. Zhu and Z. Liu, *ChemPhysChem.* 5, 998 (2004).
- [vi]. X. Zhang, Z. Lü, M. Wen, H. Liang, J. Zhang and Z. Liu, *J. Phys. Chem. B* 109, 1101 (2005).
- [vii]. J. Fan, M. Wan, D. Zhu, B. Chang, Z. Pan and S. Xie, *J. Appl. Polym. Sci.* 74, 2605 (1999).
- [viii]. G. Han, J. Yuan, G. Shi and F. Wei, *Thin Solid Films*, 474, 64 (2005).
- [ix]. G. Z. Chen, M. S. P. Schaffer, D. Coleby, G. Dixon, W. Zhou, D. J. Fray and A. H. Windle, *Adv. Mater.* 12, 7, 522 (2000).
- [x]. M. Hughes, G. Z. Chen, M. S. P. Schaffer, D. J. Fray and A. H. Windle, *Chem. Mater.* 14, 1610 (2002).
- [xi]. M. Hughes, G. Z. Chen, M. S. P. Schaffer, D. J. Fray and A. H. Windle, *Compos. Sci. Technol.* 64, 2325 (2004).
- [xii]. G. A. Snook, G. Z. Chen, D. J. Fray, M. Hughes and M. Shaffer, *J. Electroanal. Chem.* 568, 135 (2004).
- [xiii]. C. Zhou, S. Kumar, C. D. Doyle and J. M. Tour, *Chem. Mater.* 8, 1997 (2005).
- [xiv]. C. A. Dyke, and J. M. Tour, *J. Am. Chem. Soc.* 125, 1156 (2003).
- [xv]. A. Morrin, O. Ngamna, A. J. Killard, S. E. Moulton, M. R. Smyth and G. G. Wallace, *Electroanalysis* 17, 423 (2005).
- [xvi]. C. A. Dyke and J. M. Tour, *Chem. Eur. J.* 10, 812 (2004).
- [xvii]. C. A. Dyke and J. M. Tour, *J. Phys. Chem. A*, 108, 11151 (2004).
- [xviii]. V. Skakalova, A. B. Kaiser, U. Dettlaff-Weglikowska, K. Hrnčarikova and S. Roth, *J. Phys. Chem. B*, 109, 7174 (2005).
- [xix]. Y. Hu, R. Yang, D. F. Evans and J. H. Weaver, *Phys. Rev. B*, 44, 13660 (1991).
- [xx]. D. K. Grant, K. W. Jolley, D. L. Officer, K. C. Gordon and T. M. Clarke, *Org. Biomol. Chem.* 10, 2008 (2005).
- [xxi]. <http://www.sigmaaldrich.com/sigma/enzyme%20assay/a1888enz.pdf>

-----  
Na

H<sub>2</sub>SO<sub>4</sub>

NaNO<sub>2</sub>  
60°C

n

+

SWNT